Cell-laden microengineered pullulan methacrylate hydrogels promote cell proliferation and 3D cluster formation

Hojae Bae[a,b,†], **Amir F. Ahari**[a,b,†], **Hyeongho Shin**[a,c,†], **Jason W. Nichol**[a,b], **Che B. Hutson**[a,b], **Mahdokht Masaeli**[a,b], **Su-Hwan Kim**[a,b,d], **Hug Aubin**[a,b], **Seda Yamanlar**[a,b], and **Ali Khademhosseini**[a,b,*]

[a] Center for Biomedical Engineering, Department of Medicine, Brigham and Women's Hospital, Harvard Medical School, 65 Landsdowne Street, Rm 252, Cambridge, MA, 02139, USA

[b] Harvard-MIT Division of Health Sciences and Technology, Massachusetts Institute of Technology, Cambridge, MA, 02139, USA

[c] Department of Materials Science and Engineering, Massachusetts Institute of Technology, Cambridge, MA, 02139, USA

[d] Department of Biomedical Engineering, College of Health Science, Korea University, Jeongneung-dong, Seongbuk-gu, Seoul, 136-703, Republic of Korea

Abstract

The ability to encapsulate cells in three-dimensional (3D) environments is potentially of benefit for tissue engineering and regenerative medicine. In this paper, we introduce pullulan methacrylate (PulMA) as a promising hydrogel platform for creating cell-laden microscale tissues. The hydration and mechanical properties of PulMA were demonstrated to be tunable through modulation of the degree of methacrylation and gel concentration. Cells encapsulated in PulMA exhibited excellent viability. Interestingly, while cells did not elongate in PulMA hydrogels, cells proliferated and organized into clusters, the size of which could be controlled by the hydrogel composition. By mixing with gelatin methacrylate (GelMA), the biological properties of PulMA could be enhanced as demonstrated by cells readily attaching to, proliferating, and elongating within the PulMA/GelMA composite hydrogels. These data suggest that PulMA hydrogels could be useful for creating complex, cell-responsive microtissues, especially for applications that require controlled cell clustering and proliferation.

Introduction

The field of tissue engineering[1] aims to solve the problems of organ failure and donor shortages by generating approaches for controlling cell behavior[2] and to build transplantable tissues.[3,4] In the body, extracellular matrix (ECM) serves to organize cells into tissues by providing adhesion sites, signaling cues, and acting as a reservoir for growth factors.[5,6] These characteristics of the ECM are vital to the rational design of biomaterial scaffolds for tissue engineering and regenerative medicine applications.

Engineered hydrogels that can mimic the native cellular ECM have increasingly become a major research focus in tissue engineering.[3,4] Hydrogels are three-dimensional (3D) crosslinked polymer networks with high water content similar to natural tissues, making

alik@rics.bwh.harvard.edu.
[†]Authors contributed equally to this work.

hydrogels an attractive candidate for tissue engineered scaffolds and ECM analogues.[7,8] Hydrogels can also be used to control the microarchitecture in engineered tissues through the use of photopatterning and microfabrication techniques.[9–11] For example, hydrogel building blocks have been shown to be useful for constructing engineered tissues with controlled microarchitectural features.[10–13] Given their increasing use as tissue engineered scaffolds, the development of novel hydrogels that can enable cellular encapsulation and tissue formation may be of benefit.

Pullulan, a fungal exopolysaccharide, is produced from starch by *Aureobasidium pullulans*[14,15] and is a water soluble, neutral linear polysaccharide consisting of α-1,6-linked maltotriose residues.[16] The molecular weights of pullulan range from thousands to 2,000,000 Daltons (Da) depending on the growth conditions.[16] Pullulan is biodegradable[17,18] and has high adhesion, structural flexibility and solubility because of its unique linkage pattern.[19] It is also hemocompatible, non-immunogenic, non-carcinogenic, and FDA approved for a variety of applications.[15,20,21] Recently, pullulan has been investigated for use in various biomedical applications such as drug and gene delivery,[16] tissue engineering,[22] and wound healing.[16] However, while pullulan possesses many of the properties that suggest its use as a biomedical scaffold, to our knowledge pullulan hydrogels have not been previously used for tissue culture applications.

We hypothesized that pullulan-based hydrogels could be created by substituting methacrylate groups for the hydroxyl groups of pullulan to synthesize a UV crosslinkable hydrogel, pullulan methacrylate (PulMA).[23,24] We further hypothesized that based on the properties of pullulan and methacrylate chemistry that PulMA can potentially be used for cell encapsulation and be successfully micropatterned into a variety of shapes and configurations for tissue engineering applications.[16,25,26] In this report, we investigated the mechanical properties and swelling ratios of PulMA hydrogels, and the embedded cell viability[26–28] and morphology within PulMA microgels. In addition, we investigated mixing PulMA with gelatin methacrylate (GelMA)[29–31] to enhance cell adhesion, proliferation, and elongation properties of PulMA.[26]

Materials and methods

Materials

Pullulan (MW ~200,000) was purchased from Tokyo Chemical Industry (TCI). Gelatin (Type A, 300 bloom from porcine skin), methacrylic anhydride (MA) and 3-(trimethoxysilyl)propyl methacrylate (TMSPMA) were purchased from Sigma-Aldrich (St Louis, USA). Glass slides and coverslips were purchased from Fisher Scientific (Philadelphia, USA). Printed photomasks were purchased from CADart (Washington, USA), while the UV light source used (Omnicure S2000) was manufactured by EXFO Photonic Solutions Inc. (Ontario, Canada). Spacer thickness was measured with electronic digital micrometer calipers (Marathon Watch Company Ltd, Ontario, Canada).

Methacrylated pullulan synthesis

Pullulan was methacrylated as previously described.[30,31] Briefly, pullulan was mixed at 2.5% (w/v) into distilled water at room temperature and stirred until fully dissolved. MA (Sigma) was added and reacted with pullulan on ice for 24 h. The pH of the solution was kept at 8 with 5 N NaOH. The solution was dialyzed (MW cutoff 6k–8k Da) for 48 h, and lyophilized to yield methacrylated pullulan. To modify the degree of methacrylation, we added varying amounts of MA (*i.e.* 0.25%, 0.5% and 1.5% (v/v)).

Methacrylated gelatin synthesis

GelMA was synthesized as previously described.[30,31] Gelatin was mixed at 10% (w/v) with Dulbecco's phosphate buffered saline (DPBS; Invitrogen) at 50 °C and stirred until completely dissolved. The "high" degree of methacrylation was achieved by adding 20% (w/v) of MA to the synthesis reaction as previously shown.[30,31] MA was added at a rate of 0.5 mL min^{-1} under stirred conditions at 50 °C and allowed to react for 2 hours. Following a 5× dilution with DPBS to stop the reaction, the mixture was dialyzed against distilled water using 12–14 kDa cutoff dialysis tubing for 1 week at 40 °C to remove salts and methacrylic acid. The solution was lyophilized for 1 week to generate white porous foam and was stored at −80 °C. We have previously shown that a 2 hour incubation of gelatin in 20% (w/v) of MA consistently results in 80% methacrylation of gelatin.[30]

^{1}H NMR and FTIR

^{1}H-NMR spectra of pullulan and methacrylated pullulan were obtained in D_2O on a Varian Inova-500 NMR spectrometer. The degree of methacrylation was calculated by the peaks at 1.8–2.0, 5.7–5.9, 6.1–6.3 ppm from methacrylate group and the peaks at 3.3–4.1, 4.9–5.0, 5.2–5.5 ppm from pullulan. The degree of methacrylation was defined as the ratio of methacrylate groups divided by the free hydroxyl groups prior to the methacrylation reaction. FT-IR analysis was performed on a Bruker Alpha FT-IR spectrometer.

Hydrogel preparation and characterization

To generate hydrogels, freeze dried PulMA macromer was mixed into DPBS containing 0.5% (w/v) 2-hydroxy-1-(4-(hydrox-yethoxy)phenyl)-2-methyl-1-propanone (Irgacure 2959, CIBA Chemicals) as a photoinitiatior at 80 °C until fully dissolved.

Mechanical testing

Two hundred microlitres of PulMA solution was pipetted between two glass coverslips separated by a 1 mm spacer and exposed to ~4 mW cm^{-1} UV light (360–480 nm) for 150 s. Samples were detached from the slide and incubated free floating at 37 °C in DPBS for 24 h. Immediately prior to testing, an 8 mm disc was punched from each swollen hydrogel sheet using a biopsy punch. The disc was blotted lightly with a KimWipe and tested at a rate of 20% strain per min on an Instron 5542 mechanical tester. The compressive modulus was determined as the slope of the linear region corresponding with 0–5% strain.

Swelling ratio

Polymerization was performed as described for mechanical testing. Immediately following hydrogel formation, an 8 mm radius disc of each composition was punched from a flat thin sheet and placed in DPBS at 37 °C for 24 h. Discs were removed from DPBS and blotted with a KimWipe to remove the residual liquid and the swollen weight was recorded. Samples were then lyophilized and weighed once more to determine the dry weight of polymer. The mass swelling ratio was then calculated as the ratio of wet mass to the mass of dry polymer.

Cell culture

Immortalized human umbilical vein endothelial cells (HUVEC; a generous gift from the late Dr J. Folkman, Children's Hospital, Boston) constitutively expressing green fluorescent protein (GFP) were maintained in endothelial basal medium (EBM-2; Lonza) and supplemented with endothelial growth BulletKit (Lonza) in a 5% CO_2 atmosphere at 37 °C. Cells were passaged approximately twice per week and media were exchanged every 2 days. NIH 3T3 fibroblasts were maintained in DMEM supplemented with 10% FBS in a 5% CO_2 atmosphere at 37 °C and passaged twice per week. HepG2 cells were maintained in DMEM

supplemented with 10% FBS in a 5% CO_2 atmosphere at 37 °C and passaged twice per week. HUVEC cells were used for surface seeding experiments as a model to assess the ability to create endothelialized, microvascular networks, while NIH 3T3 fibroblasts and HepG2s were employed to investigate 3D encapsulated cell viability as described previously.[30]

Cell adhesion

For cell adhesion studies, square hydrogel sheets (1 cm (*w*) × 1 cm (*l*) × 300 μm (*h*)) were prepared in a similar manner as that used for mechanical testing onto TMSPMA coated glass slides. Slides were covered with a HUVEC suspension containing 5×10^6 cells mL^{-1} to a depth of approximately 1 mm above the surface of the hydrogel and incubated for 12 h prior to washing twice with DPBS, to investigate the ability of HUVEC cells to endothelialize the hydrogel surface as performed previously.[30] Media was changed every 12 h for 2 days. GFP fluorescence was visualized using an inverted fluorescence microscope (Nikon TE 2000-U) equipped with a GFP filter cube. GFP images were used to quantify total cell area using NIH ImageJ software.

Cell encapsulation

NIH 3T3 fibroblasts were trypsinized and resuspended in PulMA prepolymer containing 0.5 wt% photoinitiator at a concentration of 5×10^6 cells mL^{-1}. Microgel units (500 μm ¯ × 500 μm × 300 μm) were fabricated using a photomask[10] to investigate the viability and general cell behavior within the hydrogel over time as demonstrated previously.[13,30] One-hundred micolitres of pre-polymer solution containing NIH 3T3 fibroblasts were pipetted onto a TMSPMA treated slide and exposed to ~4 mW cm^{-2} UV light (360–480 nm) for 150 s through a patterned photomask. The glass slides containing microgels were washed with DPBS and incubated for 48 h in 3T3 medium under standard culture conditions, with the media being changed every 12 h. A calcein-AM/ethidium homodimer Live/Dead assay (Invitrogen) was used to quantify cell viability within the microgels according to the manufacturer's instructions. HepG2 cell containing PulMA hydrogels was fabricated using the same method and used for confocal image analysis.

Cell aggregate diameter measurement

For cell aggregate diameter measurements, square hydrogel sheets (1 cm (*w*) × 1 cm (*l*) × 300 μm (*h*)) containing cells were prepared on TMSPMA coated glass slides. To encapsulate cells in the PulMA hydrogels, 3T3 fibroblasts were trypsinized and resuspended in PulMA prepolymer containing 0.5 wt% photoinitiator at a concentration of 5×10^6 cells mL^{-1}. The glass slides containing microgels were washed with DPBS and incubated for 48 h in 3T3 medium under standard culture conditions, media was changed every 12 h for 7 days. Cell aggregates were visualized using an inverted fluorescence microscope (Nikon TE 2000-U). Phase contrast images were used to measure the cell aggregate diameter using Spotlight (V5.0) software.

Immunocytochemical staining

Samples from cell aggregate diameter measurement were used for immunocytochemical staining. After 3 days, cells were fixed and stained with 4% paraformaldehyde for 20 min, washed three times with PBS, followed by permeabilization with 0.1% Triton X-100, and blocking of nonspecific binding by incubation with 10% (w/v) normal goat serum in PBS. The primary antibody, anti-vinculin (abcam) was diluted at 1: 100 with 4% BSA solution, and was incubated overnight at 4 °C. The secondary Rhodamine conjugated antibody (abcam) was incubated for 1 h at room temperature. The cells were counterstained with DAPI to visualize the cell nucleus.

Confocal image analysis

After 1, 3, and 5 days in culture, HepG2 cells that were encapsulated in hydrogels were fixed with paraformaldehyde and stained with phalloidin (Alexa-Fluor 594, Invitrogen) and To-Pro3 according to the manufacturers instructions to visualize filamentous F-actin and cell nuclei, respectively. The constructs were subsequently visualized with an inverted fluorescence microscope (Nikon TE 2000-U) for phase contrast images and a confocal microscope (Leica SP5) for fluorescence images. A 150 μm z-plane was scanned with images taken every 5 μm.

Data analysis

Data were analyzed using Student's t-test or one-way analysis of variance (ANOVA). Data are presented as mean ± standard deviation. All analyses were conducted with GB-STAT software (Dynamic Microsystems, Silver Spring, MD). The level of significance was set at $p < 0.05$.

Results

Degree of methacrylation

To synthesize PulMA polymers with different degrees of methacrylation, we varied the concentration of MA in the PulMA synthesis reaction (Fig. 1A). FT-IR spectroscopy confirmed the methacrylation of pullulan (Fig. 2C), while the methacrylation degree was directly quantified by ^{1}H-NMR spectroscopy by comparing the integrated intensity of the double bond peak to that of the pullulan backbone (Fig. 2A and B).[23] By adding 0.25%, 0.5% and 1.5% (v/v) MA to the synthesis reaction we created three different batches of PulMA polymers with low (3.6%), medium (6.4%) and high (16.5%) degrees of methacrylation, respectively, demonstrating the ability to create customized PulMA polymers. The three batches of PulMA were subsequently used in the remainder of the experiments to characterize the physical and biological properties of PulMA. To create hydrogel networks, PulMA was crosslinked by using UV irradiation in the presence of a photoinitiator (Fig. 1B).

Mechanical properties

The biomechanical properties of the ECM have great influence on cell viability, function and differentiation.[32,33] To characterize the mechanical properties of the synthesized PulMA hydrogels we applied unconfined compression on UV polymerized gels for 5% (w/v) polymer concentration, for each methacrylation group respectively and analyzed the resulting compressive stress–strain properties. Increasing the degree of methacrylation increased the stiffness at all strain levels as demonstrated in the representative stress–strain curve for the 5% (w/v) PulMA (Fig. 3A). In-depth quantitative analysis showed a significant increase of the compressive modulus with increasing methacrylation degree, with values ranging between 82.8 ± 8.0 kPa, 20.3 ± 1.6 kPa, and 3.6 ± 0.9 kPa for 5% (w/v) high, medium, and low methacrylated PulMA respectively (Fig. 3B). As expected, maintaining a constant degree of methacrylation while increasing the PulMA polymer concentration (3, 5, and 10%) significantly increased the compressive modulus. Fig. 3C shows a graph for PulMA with medium methacrylation degree and increasing concentration of PulMA. As expected, increasing the concentration of PulMA resulted in a higher overall compressive modulus.

Swelling characteristics

The swelling characteristics of polymer networks are crucial to solute diffusion, surface properties, mechanical properties, and surface mobility.[34] The pore size of a polymer

network and the interaction between the polymer and the solvent will determine the degree of swelling.[10] Since hydration has a substantial effect on the physical properties of the gel as well as on the fidelity of the desired microengineered shapes, we investigated the mass swelling ratio of PulMA relative to the polymer concentration and the degree of methacrylation. To do this, UV polymerized medium methacrylation degree of 3%, 5% and 10% (w/v) PulMA as well as 5% gels with low, medium, and high methacrylation degrees were allowed to reach equilibrium over a 24 h incubation in PBS at room temperature, after which the mass swelling ratio for each gel (wet to dry mass ratio) was determined and analyzed (Fig. 4). Consistent with the mechanical data, at a constant polymer concentration the mass swelling ratio significantly increased with decreasing the degree of methacrylation (Fig. 4A). One-way ANOVA revealed a statistically significant difference between groups for the swelling ratio ($p < 0.0001$). Interestingly, there was no effect of polymer concentration on the swelling ratio in our studies. However, the data showed a trend to decreased swelling ratio with increased PulMA polymer concentrations (Fig. 4B). As swelling has a profound effect on the overall shape of the resulting hydrogels, particularly for microscale gels, these data suggest that intricate pattern fidelity could be improved by increasing the degree of methacrylation and, to a lesser degree, increasing the hydrogel percentage of PulMA.

Cell adhesion and proliferation on surfaces of PulMA gels

Cell adhesion and proliferation are important aspects of scaffolds in tissue engineering.[35] To evaluate the surface adhesion characteristics of PulMA hydrogels, we seeded GFP-labeled HUVECs on square hydrogel sheets at a density of 5×10^6 cells mL^{-1}. HUVECs were chosen because of their human origin as well as for being an established model cell type for vascularized tissue engineering applications. From the mechanical compression, swelling experiments and preliminary micropatterning experiments we determined that PulMA with a medium degree of methacrylation would be the most suitable candidate for future tissue engineering applications, as it balanced a high degree of swelling and mechanical stability. We therefore used this formulation for all the subsequent cell seeding and encapsulation studies.

To analyze the adhesiveness of the PulMA hydrogels cells were seeded on the hydrogels and the degree of adhesion was analyzed. Surfaces of PulMA hydrogels, regardless of polymer concentration, showed little cell adhesion and proliferation of HUVEC cells after 24 h incubation. To improve cell adhesion, we added various amounts of gelatin methacrylate (GelMA) to the PulMA while keeping the total polymer concentration constant (Fig. 5A). GelMA is a biodegradable and cell-responsive hydrogel previously shown as a useful gel for microengineering applications.[30,31] HUVEC surface adhesion and proliferation, measured by area of confluency after 12 h, significantly increased with the addition of 5% and 10% (w/v) of GelMA to a total PulMA–GelMA polymer concentration of 15% (w/v) by roughly 10-fold as compared to PulMA alone ($p < 0.05$) (Fig. 5C and D). However, the levels of confluency of the composite hydrogels showed no statistical difference between each other and were significantly less than GelMA alone at the same total polymer concentration ($p < 0.0001$) (Fig. 5F). Interestingly, composite hydrogels with increased PulMA concentration displayed cell morphology contrary to pure GelMA hydrogels. Increased PulMA concentration seemed to drive the HUVEC cells to form large cell aggregates (Fig. 5C) while increased GelMA seemed to lead to fewer and smaller cell aggregates and more planar and elongated cells (Fig. 5D) eventually leading to the completely elongated cell morphology of GelMA alone (Fig. 5E). These data not only suggest that cell adhesion and proliferation properties of PulMA can be tuned with the addition of GelMA, but also that PulMA could be used in composite hydrogels to tune cell morphology and aggregation.

3D cell encapsulation in PulMA micropatterns

To employ microengineered PulMA patterns as hydrogel based 3D ECM templates suitable for tissue engineering applications, cells encapsulated in PulMA gels must remain viable and functional. Similar to the previous 2D cell studies we encapsulated cells in 3D PulMA hydrogels to assess cell viability, cell morphology and cell behavior over time using PulMA with a medium degree of methacrylation at encapsulation density of 5×10^6 cells mL^{-1}. For the following encapsulation studies we used NIH 3T3 fibroblasts as a model cell line.

Cells encapsulated in 10% (w/v) PulMA and micropatterned into intricate shapes showed high pattern fidelity (Fig. 6A and B). Additionally, cell viability for fibroblasts encapsulated in 500 μm (w) × 500 μm (l) × 300 μm (h) microgels demonstrated high initial cell viability at 24 h (94.3 ± 2.3% viable cells) and at 48 h (87.9 ± 4.3% viable cells) only decreasing slightly over time (Fig. 6C and D). The high initial cell viability combined with the high pattern fidelity demonstrated PulMA's high potential for use as a cell-laden hydrogel for microscale tissue engineering applications. Optimization of photoinitiator concentration and UV exposure duration could further produce even higher initial cell viability.

Similar to the cell behavior of cells seeded onto high percentage PulMA composite hydrogel surfaces, fibroblasts encapsulated in 15% (w/v) PulMA started to form multiple cell aggregates after 24 h of culture, while individual cells remained rounded showing no elongation or spreading (Fig. 7A). While cells encapsulated in pure GelMA quickly started spreading to form elongated cell networks (Fig. 7B), adding GelMA to the PulMA hydrogels at a 1:1 ratio decreased cell aggregate formation displaying fewer and smaller aggregates and increased individual cell spreading and elongated cell network formation inside the composite hydrogel (Fig. 7C). The initial 24 h cell viability of cells encapsulated in GelMA, PulMA and composite hydrogels was comparable with over 94% of viable cells in all groups (Fig. 7D). These data suggest that, analogous to the 2D surface attachment experiments, cell behavior and morphology of cells encapsulated in 3D composite PulMA–GelMA hydrogels could be manipulated by varying the polymer ratios driving cells to form multiple cell aggregates or elongated cell networks respectively, while maintaining high cell viability.

Interestingly, the cell aggregates significantly increased in size over time (Fig. 8A and D). The mean aggregate diameter of cells encapsulated in 15% (w/v) PulMA hydrogels at 24 h was 54.8 ± 6.0 μm increasing to 88.8 ± 7.7 μm at day 3 and to 138.8 ± 8.0 μm at day 7 ($p <$ 0.0001) (Fig. 8B). Apart from multiple cell aggregates fusing together and recruiting surrounding individual cells, the total cell number appeared to increase suggesting that cell proliferation inside the aggregates played a substantial role in the aggregate diameter increase over time. In addition to the cell aggregates retaining high viability after 7 days of culture, cells inside the aggregates formed extensive cell networks with cell-to-cell junctions as demonstrated by multiple points of adhesion with neighboring cells shown by vinculin staining (Fig. 8C). Same experiment was done using HepG2-laden hydrogels to show cell aggregation using the cells with the intrinsic potential to self-organize into functional 3D aggregates and showed similar aggregate size increase over time (Fig. 8D).

Discussion

In this manuscript we present the use of pullulan methacrylate or PulMA hydrogels for cell culture and tissue engineering applications. PulMA hydrogels were synthesized through incorporation of methacrylate groups following reaction with methacrylic anhydride using similar techniques to those published previously.[24,30,36–38] Characterization of PulMA, including micropatterning properties, demonstrated similar behavior to other naturally derived, photopolymerizable hydrogels such as GelMA and methacrylated hyaluronic acid (MeHA), which have been used extensively for cell-based applications.[30,37,38] Through

modulation of the hydrogel concentration and the degree of methacrylation, a wide range of mechanical properties was achieved demonstrating the ability to tune the properties for many diverse applications and cell/tissue types while maintaining excellent cell viability. Similarly, PulMA demonstrated the ability to easily form co-polymers with other acrylated polymers, in this case with GelMA, suggesting further versatility and tunability based on the wide variety of acrylated hydrogels currently used in biomedical applications.

The physical properties of PulMA were demonstrated to be highly tunable ensuring potential usage in a wide range of applications. Through variation of the degree of methacrylation and the hydrogel concentration, the mechanical properties of PulMA were shown to be tunable between 3.6 ± 0.9 kPa and 82.8 ± 8.0 kPa. As reported by Levental *et al.*, this range is similar to the native properties of a number of tissue types, such as skeletal and cardiac muscle, liver, lung and kidney, suggesting that PulMA could be appropriate for fabricating many different engineered tissues.[39] In addition, the combination of specific mechanical properties and microarchitecture have been shown to be vital to recapitulating the stem cell niche to control stem cell behavior,[33,40] suggesting that microfabricated PulMA with tunable mechanical properties could be a useful tool in stem cell-based applications and engineered tissues.[27,41] Many hydrogel materials, synthetic (*e.g.* PEG), ECM-based (*e.g.* collagen, fibrin, Matrigel), or modified natural materials (*e.g.* GelMA, HA) have mechanical properties that fall within the range of native tissues, which explain their extensive use.[39] However, in comparison with other acrylated hydrogels, PulMA showed strong long term viability for encapsulated cells, with suggested evidence of cell proliferation and organization, neither of which occur appreciably in PEG or HA. GelMA demonstrated similar long term encapsulated cell viability with extensive cell proliferation and reorganization, unlike in PulMA, however, the range of mechanical properties is much lower than for PulMA, limiting its use for applications where greater mechanical strength is required.[30] In addition, higher order cellular organization was unique in PulMA as compared to other hydrogels making it suitable for applications where other hydrogels are not well-suited.

The ability to control and regulate cell aggregate formation in 3D is critical to creating reproducible techniques for investigation of cell behaviors, such as cell differentiation, fate and proliferation. For example, embryoid body (EB) dimensions have been demonstrated to be a crucial factor in controlling embryonic stem cell differentiation, therefore a simple system for reliably creating aggregates of controlled size could be of great value to such applications.[42] Aggregate encapsulation, and sometimes proliferation, has been demonstrated in hydrogels such as alginate[43,44] and PEG.[3,4,45,46] Encapsulation of aggregates in PEG was possible by performing cell cluster formation prior to encapsulation, with the PEG matrix maintaining cell viability while restricting further cluster growth.[45,46] Aggregate formation and growth were possible in alginate based systems,[44,45] and with PEG modified with cell-degradable motifs,[3,4] however, the lack of photocrosslinking greatly limits the ability to create microarchitectural features. Furthermore, as evidenced in results using PEG modified with both RGD binding and MMP degradable motifs, if cells have the ability to bind to the matrix, they often migrate away from the clusters rather than expanding in controlled fashion. Therefore, the ideal hydrogel for aggregate formation and maintenance must enable cluster expansion without allowing for extensive cell migration.

The unique properties of PulMA enabled the ability to create 3D aggregates of controlled size simply through encapsulation of suspended cells.[26] The average aggregate diameter was shown to vary significantly with time from ~50 to 150 μm in 15% (w/v) PulMA, suggesting that an even wider range and greater control could be achieved by determining the optimal degree of methacrylation, hydrogel concentration, initial cell density and culture time to achieve the desired aggregate size and cell aggregate behavior while maintaining high

viability. The ability to create high fidelity, cell-laden micropatterns in PulMA using standard photolithography techniques while maintaining high cell viability is of benefit for this and other microscale tissue engineering applications. This also suggests that PulMA may be suited for creating engineered tissues where controlled cell aggregation is important, such as in the liver and pancreas. Further coordination between micropattern geometry and hydrogel parameters could enable even greater control of aggregate geometry and the resultant properties,[47] while optimization of potential co-polymer components, such as GelMA, could enable interconnection of the aggregates to improve cluster-to-cluster communication.

Conclusion

In this report we synthesized PulMA hydrogels and demonstrated their use for cell culture and tissue engineering applications, highlighting the properties that make PulMA an attractive material for creating cell-laden microtissues. The physical properties of PulMA were demonstrated to be controllable by changing the degree of methacrylation and the gel concentration to yield a tunable range of mechanical and swelling properties for different applications. PulMA was easily patterned with the fidelity and robustness needed to fabricate a cell-laden microgel or as a microfluidic device, similar to other commonly used hydrogels. Furthermore, cells proliferated within PulMA forming organized, 3D aggregates, the size of which changed as a function of time. The integration of gelatin with PulMA was also shown as a method of further enhancing its biological properties. These data suggest that PulMA could be used for various applications, especially for applications where control of cell aggregation is important, such as hepatic and embryonic stem cell culture.

Acknowledgments

References

1. Langer R, Vacanti JP. Science 1993;260:920–926. [PubMed: 8493529]

2. Nelson CM, Chen CS. FEBS Lett 2002;514:238–242. [PubMed: 11943158]

3. Lutolf MP, Lauer-Fields JL, Schmoekel HG, Metters AT, Weber FE, Fields GB, Hubbell JA. Proc Natl Acad Sci U S A 2003;100:5413–5418. [PubMed: 12686696]

4. Lutolf MP, Weber FE, Schmoekel HG, Schense JC, Kohler T, Muller R, Hubbell JA. Nat Biotechnol 2003;21:513–518. [PubMed: 12704396]

5. Lanza, R.; Langer, R.; Vacanti, J. Principles of Tissue Engineering. 2. Academic Press; 2000. p. 237-250.

6. Patterson J, Martino MM, Hubbell JA. Mater Today (Oxford, U K) 2010;13:14–22.

7. Drury JL, Mooney DJ. Biomaterials 2003;24:4337–4351. [PubMed: 12922147]

8. Shah DN, Recktenwall-Work SM, Anseth KS. Biomaterials 2008;29:2060–2072. [PubMed: 18237775]

9. Khademhosseini A, Eng G, Yeh J, Fukuda J, Blumling J, Langer R, Burdick J. J Biomed Mater Res A 2006;79:522–532. [PubMed: 16788972]

10. Du Y, Lo E, Ali S, Khademhosseini A. Proc Natl Acad Sci U S A 2008;105:9522–9527. [PubMed: 18599452]

11. McGuigan AP, Sefton MV. Proc Natl Acad Sci U S A 2006;103:11461–11466. [PubMed: 16864785]

12. Nichol JW, Khademhosseini A. Soft Matter 2009;5:1312–1319. [PubMed: 20179781]

13. Zamanian B, Masaeli M, Nichol JW, Khabiry M, Hancock MJ, Bae H, Khademhosseini A. Small 2010;6:937–944. [PubMed: 20358531]

14. Mulchandani A, Luong JHT, Leduy A. Biotechnol Bioeng 2004;32:639–646. [PubMed: 18587764]

15. Coviello T, Matricardi P, Marianecci C, Alhaique F. J Controlled Release 2007;119:5–24.

16. Rekha MR, Chandra PS. Trends Biomater Artif Organs 2007;20:116–121.

17. Bruneel D, Schacht E. J Bioact Compat Polym 1995;10:299–312.

18. Ball DH, Wiley BJ, Reese ET. Can J Microbiol 1992;38:324–327. [PubMed: 1611558]

19. Leathers TD. Appl Microbiol Biotechnol 2003;62:468–473. [PubMed: 12830329]

20. Kimoto T, Shibuya T, Shiobara S. Food Chem Toxicol 1997;35:323–329. [PubMed: 9207894]

21. Leathers TD. Appl Microbiol Biotechnol 2003;62:468–473. [PubMed: 12830329]

22. Thebaud NB, Pierron D, Bareille R, Le Visage C, Letourneur D, Bordenave L. J Mater Sci: Mater Med 2007;18:339–345. [PubMed: 17323167]

23. Masci G, Bontempo D, Crescenzi V. Polymer 2002;43:5587–5593.

24. Crescenzi V, Dentini M, Bontempo D, Masci G. Macromol Chem Phys 2002;203:1285–1291.

25. Na K, Shin D, Yun K, Park KH, Lee KC. Biotechnol Lett 2003;25:381–385. [PubMed: 12882557]

26. Autissier A, Letourneur D, Le Visage C. J Biomed Mater Res, Part A 2007;82:336–342.

27. Okazaki A, Jo J, Tabata Y. Tissue Eng 2007;13:245–251. [PubMed: 17518561]

28. San Juan A, Hlawaty H, Chaubet F, Letourneur D, Feldman LJ. J Biomed Mater Res, Part A 2007;82:354–362.

29. Van Den Bulcke AI, Bogdanov B, De Rooze N, Schacht EH, Cornelissen M, Berghmans H. Biomacromolecules 2000;1:31–38. [PubMed: 11709840]

30. Nichol JW, Koshy ST, Bae H, Hwang CM, Yamanlar S, Khademhosseini A. Biomaterials 2010;31:5536–5544. [PubMed: 20417964]

31. Aubin H, Nichol JW, Hutson CB, Bae H, Sieminski AL, Cropek DM, Akhyari P, Khademhosseini A. Biomaterials 2010;31:6941–6951. [PubMed: 20638973]

32. Engler AJ, Sweeney HL, Discher DE, Schwarzbauer JE. J Musculoskeletal Neuronal Interact 2007;7:335.

33. Engler AJ, Sen S, Sweeney HL, Discher DE. Cell 2006;126:677–689. [PubMed: 16923388]

34. Peppas N, Hilt J, Khademhosseini A, Langer R. Adv Mater 2006;18:1345–1360.

35. Khademhosseini A, Vacanti JP, Langer R. Sci Am 2009;300:64–71. [PubMed: 19438051]

36. Benton JA, DeForest CA, Vivekanandan V, Anseth KS. Tissue Eng 2009;15:3221–3230.

37. Brigham MD, Bick A, Lo E, Bendali A, Burdick JA, Khademhosseini A. Tissue Eng 2009;15:1645–1653.

38. Burdick JA, Khademhosseini A, Langer R. Langmuir 2004;20:5153–5156. [PubMed: 15986641]

39. Levental I, Georges PC, Janmey PA. Soft Matter 2007;3:299–306.

40. Murtuza B, Nichol JW, Khademhosseini A. Tissue Eng, Part B 2009;15:443–454.

41. Wong VW, Rustad KC, Galvez MG, Neofytou E, Glotzbach JP, Januszyk M, Major MR, Sorkin M, Longaker M, Rajadas J, Gurtner G. Tissue Eng Part A10.1089/ten.tea.2010.0298

42. Hwang YS, Chung BG, Ortmann D, Hattori N, Moeller HC, Khademhosseini A. Proc Natl Acad Sci U S A 2009;106:16978–16983. [PubMed: 19805103]

43. Chen MCW, Gupta M, Cheung KC. Biomed Microdevices 2010;12:647–654. [PubMed: 20237849]

44. Bazou D, Coakley WT, Hayes AJ, Jackson SK. Toxicol in Vitro 2008;22:1321–1331. [PubMed: 18490133]

45. Mason MN, Mahoney MJ. Tissue Eng Part A10.1089/ten.tea.2010.0015

46. Weber LM, He J, Bradley B, Haskins K, Anseth KS. Acta Biomater 2006;2:1–8. [PubMed: 16701853]

47. Hasuda H, Kwon OH, Kang IK, Ito Y. Biomaterials 2005;26:2401–2406. [PubMed: 15585243]
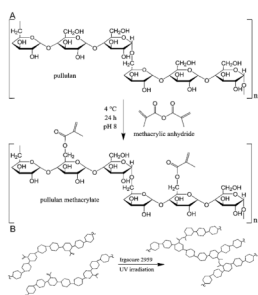
Fig. 1.
Synthesis of pullulan methacrylate (PulMA). (A) Pullulan macromers containing C-6 hydroxyl groups were reacted with methacrylic anhydride (MA) to add methacrylate pendant groups. (B) To create a hydrogel network, PulMA was crosslinked using UV irradiation in the presence of a photoinitiator.
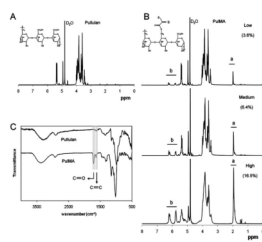
Fig. 2.
FT-IR and NMR characterization of methacrylated pullulan. (A) Representative ^{1}H NMR spectrum of pullulan. (B) Representative ^{1}H NMR spectrum of PulMA. (C) Representative FT-IR spectra of pullulan and PulMA.
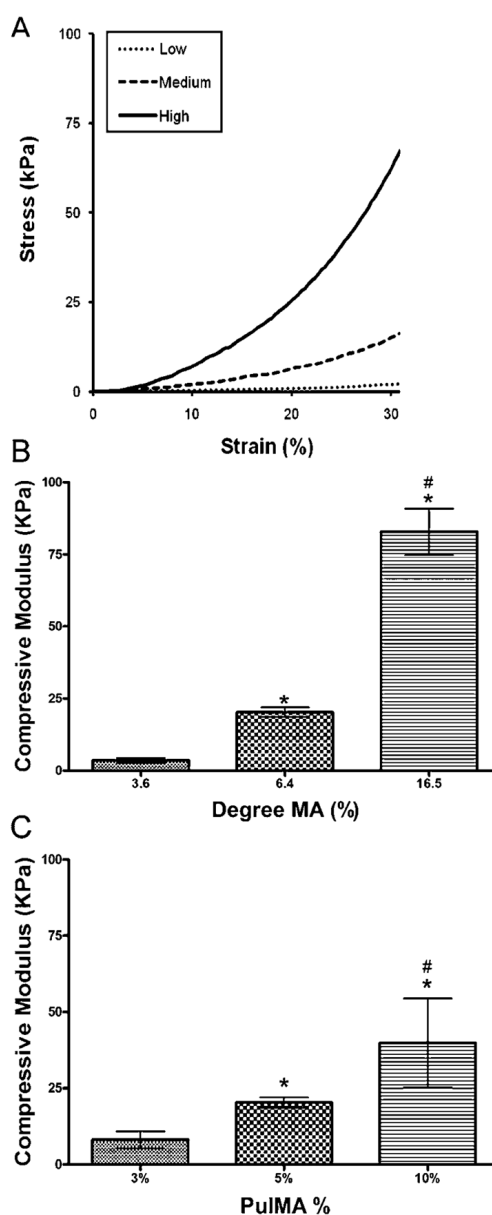
Fig. 3.
Mechanical properties of PulMA with varying concentrations or degrees of methacrylation.
(A) Representative curves from 5% PulMA at varying degrees of methacrylation. (B)
Compressive modulus for 5% (w/v) PulMA at low, medium, and high degree of
methacrylation and (C) compressive modulus for 3%, 5%, and 10% (w/v) PulMA at medium
degree of methacrylation. One-way ANOVA revealed differences between groups for the
degree of methacrylation ($p < 0.0001$) and for the percentage of PulMA ($p < 0.0001$).
Fisher's LSD $p < 0.05$: * *vs.* Low and # *vs.* Med. Fisher's LSD $p < 0.05$: * *vs.* 3% and # *vs.*
5%. Error bars represent the SD of measurements performed on 5 samples.
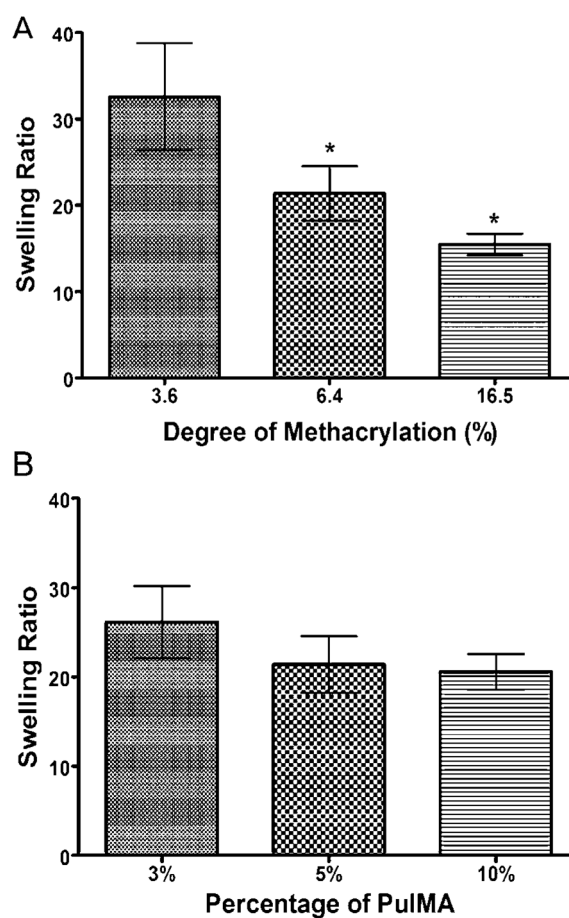
Fig. 4.
Equilibrium swelling properties of PulMA hydrogels. The mass swelling ratios of PulMA hydrogels at various PulMA % (w/v) and degrees of methacrylation. One-way ANOVA revealed differences between groups for changes in the degree of methacrylation ($p <$ 0.0001). Fisher's LSD $p <$ 0.05: * $vs.$ Low. Error bars represent the SD of measurements performed on 5 samples.
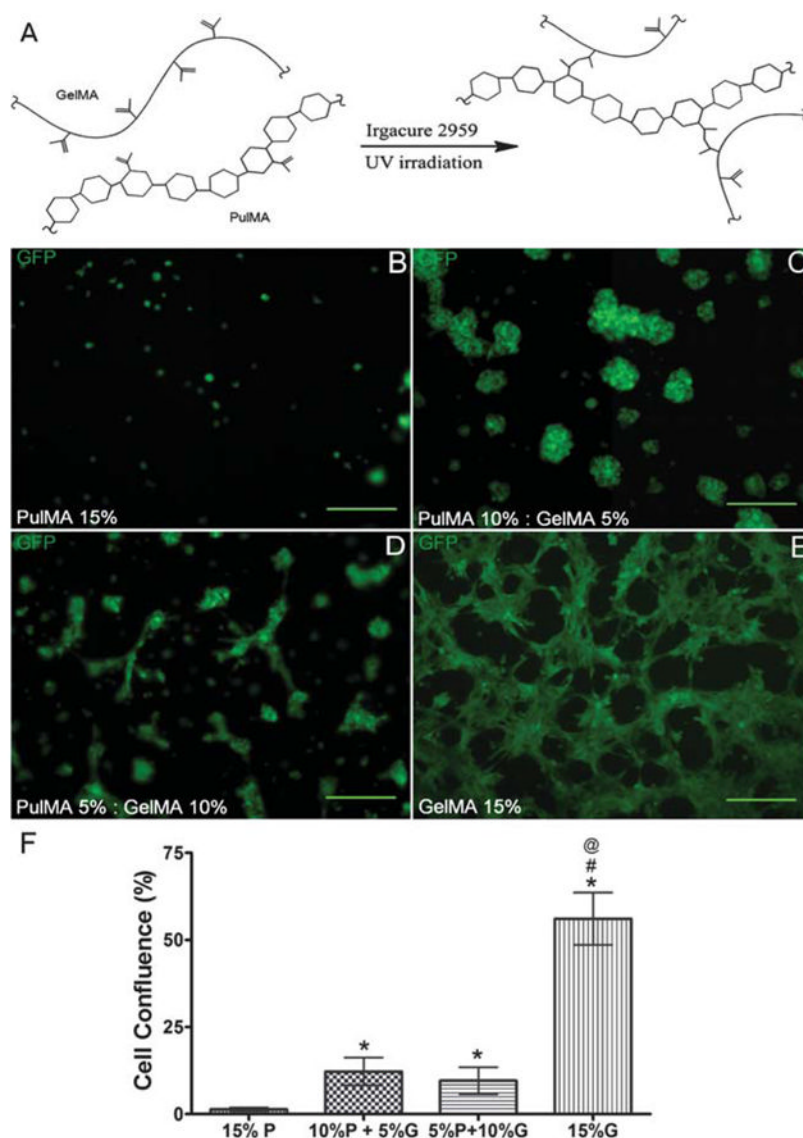
Fig. 5.
Cell adhesion on surface of PulMA, PulMA: GelMA, and GelMA hydrogels. (A) To create a PulMA–Gelatin complex hydrogel network, PulMA and GelMA were crosslinked by using UV irradiation in the presence of a photoinitiator. (B–E) GFP HUVECs readily adhered to GelMA and PulMA–GelMA, but did not adhere to PulMA alone as demonstrated by endogenous GFP (scale bar = 100 μm). (F) The percent confluency was significantly different proportional to the added GelMA percentage. Error bars represent the SD of 4 independent samples (*$p < 0.05$). Statistical analysis illustrates a difference between groups ($p < 0.0001$). Fisher's LSD $p < 0.05$: * *vs.* 15% P, # *vs.* 10% P + 5% G, and @ *vs.* 5% P + 10% G.
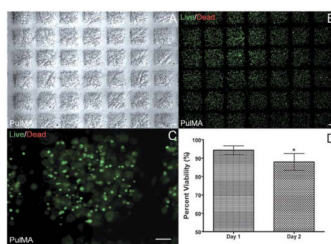
Fig. 6.
Characterization of embedded cell behavior in micropatterned PulMA (500 μm × 500 μm).
3T3 fibroblasts embedded in 10% PulMA micropatterns were stained with calcein-AM
(green)/ethidium homodimer (red) Live/Dead assay 48 h after encapsulation (scale bar = 100
μm). (A) Phase contrast and (B) Live and Dead assay (2×) images of micropatterned PulMA
(10% w/v) using photoinitiator (0.5% w/v) and UV irradiation. (C) Live and Dead assay
(10×) images of micropatterned PulMA (10% w/v) using photoinitiator (0.5% w/v) and UV
irradiation. (D) Quantification of cell viability demonstrated excellent cell survival 48 h after
encapsulation (scale bar = 100 μm) ($p < 0.05$). Error bars represent the SD of 3 independent
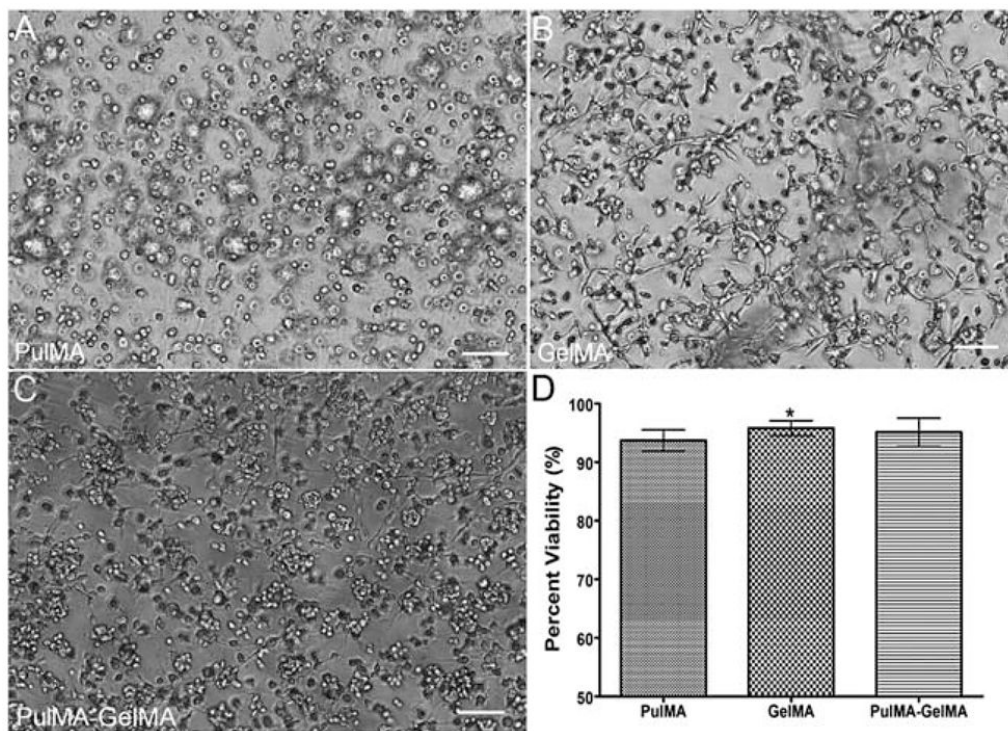samples.

Fig. 7.
Characterization of embedded cell behavior in PulMA. 3T3 fibroblasts embedded in PulMA, GelMA, and PulMA: GelMA after 24 h after encapsulation (scale bar = 100 µm). (A–C) Phase contrast images of 3T3 cultured within 15% (w/v) PulMA, 15% (w/v) GelMA, and 7.5%: 7.5% (w/v) PulMA: GelMA after 24 h. (D) Quantification of cell viability by Live/Dead assay 24 h after encapsulation demonstrated excellent cell survival at all conditions. One-way ANOVA reveals differences between groups for percent viability ($p < 0.0001$). Fisher's LSD $p < 0.05$: * *vs.* PulMA. Error bars represent the SD of 3 independent samples per condition.
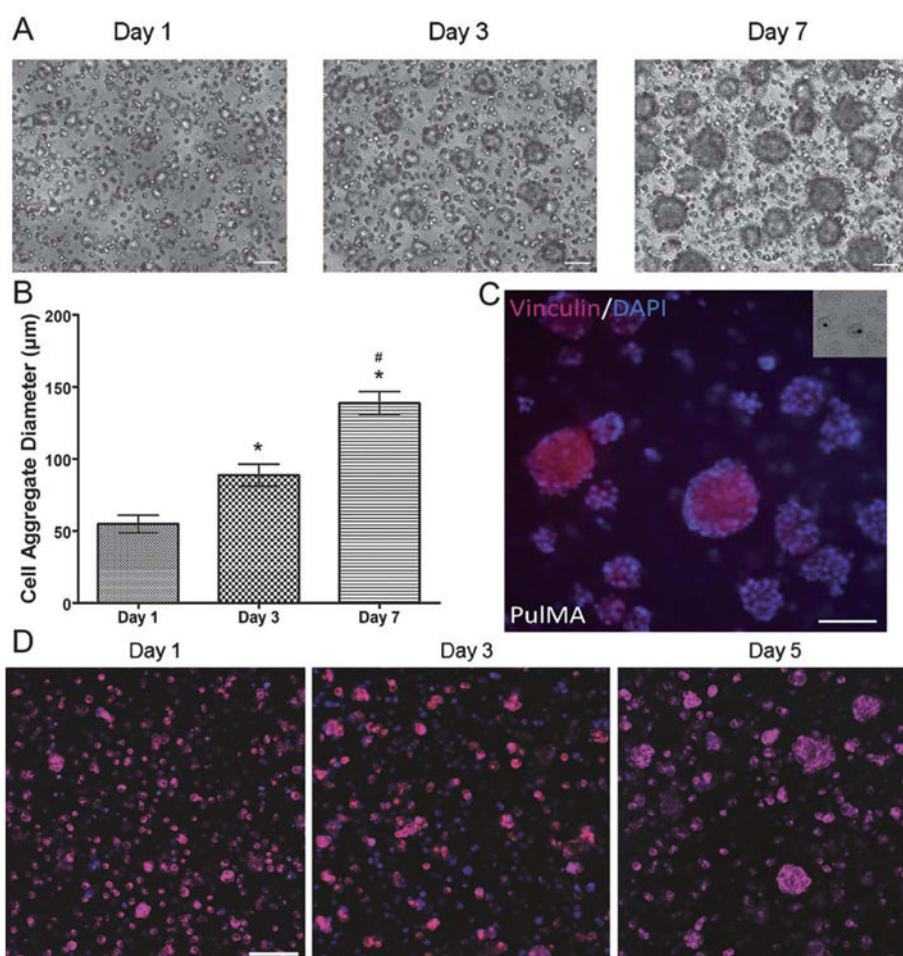
Fig. 8.
3D cell aggregate formation in PulMA hydrogels. (A) Phase contrast images of 3D cell aggregate formation of 3T3-fibroblast-laden 15% PulMA hydrogels (1 cm (*w*) × 1 cm (*l*) × 300 μm (*h*)) at day 1, 3, and 7 respectively (scale bar = 100 μm). (B) Quantification of average cell aggregate diameter at day 1, 3, and 7 respectively. (C) Immunocytochemical characterization of formed 3T3-fibroblast aggregates cell-to-cell junction after 3 days. This molecular expression was identified by anti-vinculin (red) (scale bar = 100 μm). (D) Representative To-Pro3/F-actin stained confocal images (150 μm *z*-plane) of a HepG2 containing 15% (w/v) PulMA hydrogel at day 1,3, and 5 (scale bar = 100 μm). One-way ANOVA reveals differences between groups for cell aggregate size ($p < 0.0001$). Fisher's LSD $p < 0.05$: * *vs.* Day 1 and # *vs.* Day 3. Error bars represent the SD of 3 independent samples per condition.